

RoMag Standard Operating Procedures

Jonathan Aurnou

Jonathan Cheng

Alex Grannan

Emily Hawkins

Ashna Aggarwal

Department of Earth, Planetary, and Space Sciences

University of California - Los Angeles

January 19, 2017

Contents

A. Romag Overview	4
A.1 Magnet	4
A.2 Other Design Considerations	5
B. Musculoskeletal System	6
B.1 Lower Frame	6
B.2 Bearing and Lower Table	7
B.3 Rotation System	7
B.3.1 New Rotating System	8
B.4 Upper Frame	8
C. Circulatory System	8
C.1 Wiring	8
C.1.1 The Heat Pad	9
C.1.2 Power Managment Unit (PMU)	9
C.1.3 Laboratory Frame Wiring	9
C.1.4 Slip Ring	9
C.1.5 Rotating Frame Wiring	10
C.2 Plumbing	10
C.2.1 Rooftop Chiller	10
C.2.2 Laboratory Chiller	10
C.2.3 Rotary Union	11
C.2.4 The Heat Exchanger	11
C.2.5 Flushing the Rooftop Chiller	11
C.2.6 Filling and Draining the Heat Exchanger	11
C.2.7 Filling and Draining the Laboratory Chiller	11
C.3 Troubleshooting	11
D. Gastrointestinal System	11
D.1 Fluid Properties	12
D.1.1 Fluid Properties of Water	12
D.1.2 Fluid Properties of Sucrose Solution	12
D.1.3 Fluid Properties of Gallium	12
D.2 The Tank	13
D.2.1 Cylindrical Sidewalls	14
D.2.2 The Expansion Tank	15
D.2.3 The Top and Bottom Thermal Blocks	16
D.2.4 Internal Thermistor Holders	17
D.3 Assembling the Stack	18
D.4 Troubleshooting	18
E. Water Storage, Degassing, and Filling	18
F. Gallium Storage, Cleaning, and Filling	19
F.1 Storage	19
F.2 Gallium Cleaning	19
F.3 Before the Gallium Transfer	20
F.3.1 Room	20
F.3.2 Fumehood	20
F.3.3 Transfer Hose	20
F.3.4 Experimental Stack	21
F.4 During the Filling	21
F.5 Emptying the Tank	22
F.6 Troubleshooting	22

G. DDC Alarms and Safety Controls	22
G.1 Alarm Control	22
G.2 Alarm Definitions	22
G.3 Alarm Priorities	23
G.3.1 P1: “Highest Priority”	23
G.3.2 P2: “Medium Priority”	23
G.3.3 P3: “Low Priority”	23
H. Nervous System	25
H.1 Labview Monitoring System: Front Panel	25
H.2 Labview Monitoring System: Back Panel	25
H.2.1 Gathering Channel Information	25
H.2.2 Displaying Data	25
H.2.3 Calculating Dimensional Quantities	25
H.2.4 Calculating Non-Dimensional Quantities	25
H.2.5 Sending Monitor Emails	25
H.2.6 Saving Data	25
H.3 Labview Alarms and Notifications	25
H.4 Labview Monitoring and Alarms Troubleshooting	25
H.5 Heat Pad Control	26
H.6 Lab Chiller Control	26
H.7 Roof Chiller Control	26
H.8 Rotation Control	26
H.9 Magnet Control	26
H.9.1 Raising and Lowering the Magnet	26
H.9.2 Changing the Magnetic Field	26
H.10 Lab Chiller Flow Rate Control	26
H.11 Controls Troubleshooting	26
I. Measurements	26
I.1 Measuring Rotation	26
I.2 Measuring Magnetic Field Data	26
I.2.1 Hall Probes	26
I.2.2 Magnet Current Sensor	26
I.3 Measuring Thermal Data	26
I.3.1 Thermistors	27
I.3.2 Sidewall Heat Losses	28
I.3.3 Thermocouples	28
I.4 Labview Acquisition	28
J. Acquiring Velocity Data	28
J.0.1 Doppler Velocimetry	28
K. Acquiring Flow Rate Data	31
L. Flow Visualization	31
M. Running Cases	32
N. Post-Processing Data	34
N.1 Calculating Thermal Corrections	34
N.2 Calculating Sidewall Heat Losses	34
N.3 Calculating the Average Fluid Temperature	34
N.4 Calculating the Fluid Properties	34
N.5 Calculating the Ekman Number	34
N.6 Calculating the Temperature Drop Across the Fluid Layer	35

N.7 Calculating the Rayleigh Number	35
N.8 Calculating the Nusselt Number	35
O. Post Processing Data for Path to Magnetostrophy	36

List of Figures

1 PMU Voltage Divider Wiring Diagram	10
--	----

List of Tables

1 Table of alarm definitions and locations.	22
2 Table of alarm definitions and locations.	24

A. Romag Overview

A.1 Magnet

In order to impose a magnetic field strong enough for Lorentz forces to be within the desired range, currents of nearly 100 Amps are needed. Currents of this strength must be passed through heavy gauge copper wire, and even then will generate significant heat through electrical resistance. The magnet, then, needs to be actively cooled via recirculation of thermostated water. Thus, in order to reach the magnetostrophic regime, a rather large, self-contained electromagnet is required. Our magnet has a mass of 450 kg.

The need for a large magnet is not an overwhelming difficulty per se, but in combination with rapid rotation, design complications amass. Rotating a 450 kg magnet at up to 100 RPM is a dangerous prospect. We overcome this challenge by arranging the coils of the magnet in such a way that they generate a nearly uniform, vertical magnetic field within the volume of the convection tank. This allows us to leave the magnet in the stationary lab frame while the experiment rotates through it's field. If the field is azimuthally uniform, there will be no difference between a stationary and co-rotating magnet.

An illustration of the magnet is shown in figure 4. It was fabricated by Walker LDJ and has basic dimensions 0.61 m wide by 0.61 m deep by 1.07 m high with a 0.38 m diameter hollow inner bore. The magnet has a lower base plate designed to be fitted to jack screws and a roller guide so that it can be lowered from above to encapsulate the convection tank within its inner bore (see section 2.3). The magnet coils are arranged in an upward spiraling hour-glass shape, with coil density increasing near the top and bottom of the magnet. This current distribution generates a magnetic field that is vertical within the magnet's

bore, and uniform to within 0.5% within the experimental volume. Figure 5 shows measurements of the uniformity of field strength within our working volume. The magnet is powered by a Walker Scientific HS 200-80 power supply with a PSC-3 control module. With maximum current output of 80 A, the magnet produces a 0.13 T field (see figure 6). Both the magnet and power supply need to be liquid cooled by at least 3 gallons per minute (GPM) chilled water.

Several steps are required to properly lower and raise the magnet from the high resting position and enclose the convection tank.

1. The jack screws on which the magnet is supported must be uniformly greased
2. All components of the convection tank must be horizontal. Check this with a level.
3. To begin the lowering mechanism, locate the lab’s fuse box and switch labeled “Duff-Norton.” Move to “on”
4. Move to the Duff-Norton box, and press the button labeled “Lower.” As the magnet is moving downwards, inspect the experimental components on the convection tanks (such as wires, pipes, etc.) and ensure that they are not obstructing the magnet. In particular, take note of RoMag’s lowering frame and its proximity to wires.
5. The magnet has a lower limit and it will stop being lowered at the point where the DDC lever is activated.
6. Additionally, allow room for further insulation to be placed between the tank and magnet.
7. When experimentation is complete, push the “Raise” button to lift the magnet to its original position. It will automatically stop at the top.

$$B = 1.2 + 16.0A \tag{1}$$

A.2 Other Design Considerations

Another complication introduced by the desire for a strong, uniform magnetic field is that we now require the experimental device to be constructed from non magnetic materials. In the presence of an applied field, magnetic materials will distort this field, and in so doing alter the influence of that field on our convecting fluid. Non-magnetic here then refers to a negligible amount of paramagnetism, which can be described by

a material's permeability relative to a vacuum μ/μ_0 . Non-magnetic materials have $\mu/\mu_0 \sim 1$. Steel is a classic example of a strongly magnetic material that is commonly used in experimental fabrication, with $\mu/\mu_0 = 700$. This construction limitation restricts our use to non-magnetic materials such as aluminum ($\mu/\mu_0 = 1.000022$) and copper ($\mu/\mu_0 = 0.999994$) alloys, and plastics such as Teflon (PTFE). In most high-heat applications, aluminum and copper alloys are best suited. Unfortunately, we must also account for the corrosive nature of liquid gallium in our experimental design. Both copper and aluminum react with gallium. Stainless steel (SS 316L) provides a good (albeit expensive), non-magnetic, non-reactive, high temperature alternative. All of these materials are used in different capacities in the construction of RoMag, and will be discussed further below.

One last basic design consideration I will mention before discussing the individual systems in detail is the on-board diagnostics. Information is passed from the rotating frame to the static lab frame via electrical slip rings (see section ???). Previous experiments have found difficulty in maintaining a high signal to noise ratio in certain sensors (such as acoustic Doppler transducers) when passing these signals through slip-rings, on account of the introduction of rotational noise. For this reason, RoMag has been designed to acquire data within the rotating frame. This requirement leads to the incorporation of a co-rotating lower turntable to which many of our diagnostics systems are attached in order to preserve the quality of our measurements.

B. Musculoskeletal System

B.1 Lower Frame

The musculoskeletal system of RoMag refers to its basic structure and mechanical framework. RoMags framework consists of a lower frame and an upper frame. Both are constructed from structural aluminum and painted with protective enamel to guard against corrosion by gallium.

The lower frame is shown in figure ???, and has dimensions of 0.86 m wide by 0.78m deep by 0.61m high. The lower frame supports the weight of all experimental components, and is leveled manually using thin metal shims. At the center of the top of the lower frame is a platform on which sits our bearing, which separates the rotating and stationary experimental components.

B.2 Bearing and Lower Table

The bearing is an MTO-145 Super Heavy Duty Turntable manufactured by the Kaydon Corporation, Inc., has dimensions 0.05m h 0.3 m OD 0.145 m OD, and is rated to bear a 68,000 kg load capacity. The top surface of the bearing supports a co-rotating stainless steel pedestal on which sits the convection tank. A hollow shaft is fixed to the large inner bore of the bearing, which permits the passage of fluid, electrical power and electrical signals from below to the convection tank along the devices rotation axis (see sections ??? and ???). The bottom of this shaft supports the co-rotating lower table, which allows certain diagnostic and control systems to reside in the rotating frame. The lower table is constructed from aluminum and has a diameter of 0.81 m. The top of the lower frame is amalgamated into one water-tight surface using plexiglass to prevent any convection tank spills from reaching the electronics on the lower table.

B.3 Rotation System

Rotation is driven by a brushless Kollmorgan Goldline XT servomotor, model MT502B2-R1C1. The motor can rotate with torques up to 10.1 Nm, and is connected to the bearing via a driving belt (with adjustable tension) attached to a 40:1 ratio gear head. The motor is controlled and monitored by a Kollmorgan Servostar CD servodrive, model CR06250. We connect to servodrive via RS232 serial cable using the Dell fumehood computer and Kollmorgan software, ServoStar CD, which allows us to control the rotation rate of the motor, and therefore 1/40 that of the bearing, lower table, and pedestal assembly. Typical steady rotation rates are uniform to better than 0.5%, as seen in Figure ???.

- Note: Talking to the servo with the 9pin RS232 only requires 3 lines: Data in, Data out, and Ground which corresponds to pin 2, pin 3, and pin 5 respectively on a standard RS232 connector. However the Data in/out is flipped for the servo so going from the computer to the servo you must connect pin 2 from the computer to pin 3 on the servo, pin 3 on the computer to pin 2 on the servo, and pin 5 on the computer to pin 5 on the servo. If you don't then the servo will not be recognized by the communication software.

The servodrive also monitors the rotation rate and outputs a voltage signal. This signal is currently **not** incorporated into our diagnostic system .

B.3.1 New Rotating System

A new rotating system consists of a Marathon motor and Yaskawa variable frequency drive but it is in storage and has not been implemented yet.

B.4 Upper Frame

The upper frame is also constructed from aluminum, and is intended to provide support to the magnet, which sits atop the experimental device. With the addition of the upper frame, RoMag stands at 3.3 m tall. A photograph of the assembled frame (with pedestal and magnet lift assembly) is shown in figure ???. This basic setup is shown in figure ??. The weight of the magnet is supported by the lower frame, and the upper frame provides lateral support. The magnet is raised and lowered by a lift system shown in figure ??. Three adaptor feet are affixed to the base of the magnet and threaded into 1.5 m stainless steel jack-screws. The magnet is then raised and lowered by turning the jack-screws in one direction or the other. This is accomplished by a 3/4 hp Duff-Norton gear motor (model 817MDSF), rated at 33 Nm maximum torque. The three jack-screws are linked by three worm gear actuators and two mitre boxes. Safety components of the lift system include a dynamic brake and a rotary limit switch. Raising and lowering of the magnet are aided by a long Delrin guide shaft, which stabilizes the magnet via guide rollers.

C. Circulatory System

C.1 Wiring

The circulatory system of RoMag refers to its heating and cooling system, comprised of both electrical power and coolant circulation.

Heat is required to drive convection. In order for the system to equilibrate thermally, all heat injected must be removed. This is the underlying principal of RoMags circulatory system: we aim to provide efficient conduits of energy flow beginning at our electrical power source and ending in the atmosphere. Figure ??? shows a schematic flow chart of this path. Heat is generated by passing currents through electrical resistors. This essentially occurs in three RoMag components: the convection tanks heat pad; the magnet power supply; and the magnet itself. In the former, heat is intentionally generated in an electrical resistor; in the latter two, heat generation is a byproduct of the large currents required to generate strong magnetic

fields.

C.1.1 The Heat Pad

The heater is a silicone rubber heater manufactured by OEM. The heaters conductors are non-inductively wound, i.e. arranged such that they induce negligible magnetic field. This is important in maintaining a uniform magnetic field within the convection tank. The heater has an electrical resistance of 18.66 Ohms. A direct current is passed through the heater by way of an Argantix XDS 300-17 power supply. This power supply is capable of delivering up to 300 V at 16.7 A, or up to 5010 W of power. With the power supply, we control the voltage output. It is useful then to recognize that the input heat power, P , will be

$$P = V^2/R = \frac{V^2}{6883 \text{ Ohms}} \quad (2)$$

where V and R are voltage and resistance, respectively. The heater's power supply, which is powered by three-phase 208 VAC facility power, is in the stationary lab frame. The heat pad, however, is in the rotating experimental frame.

C.1.2 Power Managment Unit (PMU)

The power managment unit (PMU) is the device for measuring the power being applied to the heat pad. Because the PXI and SCXI can only measure small voltages, it necessary to reduce the voltage going to the heat pad to a readable level, and it is necessary to use a shunt resistor with a small but well-known resistance so as to measure a small voltage drop across the shunt resistor and compute the resulting current going through the shunt resistor and thus the heat pad. The measurements of the resistors in the voltage divider has measured by the Agilent meter is $R_1 = 300K\text{Ohms}$, $R_2 = 10K\text{Ohms}$, $R_{shunt} = ????\text{Ohms}$

C.1.3 Laboratory Frame Wiring

C.1.4 Slip Ring

This heating current, then, must be passed through electrical slip-rings into the rotating frame. The slip-rings are manufactured by Poly-Scientific (of Northrup Grumman), model AC6098-24. The slip rings have a 0.2m outer diameter, and a 0.1m diameter hollow inner bore. This allows the slip-rings to be situated outside the rotating shaft, between the lower rotating table and the main bearing. The solid state slip-rings

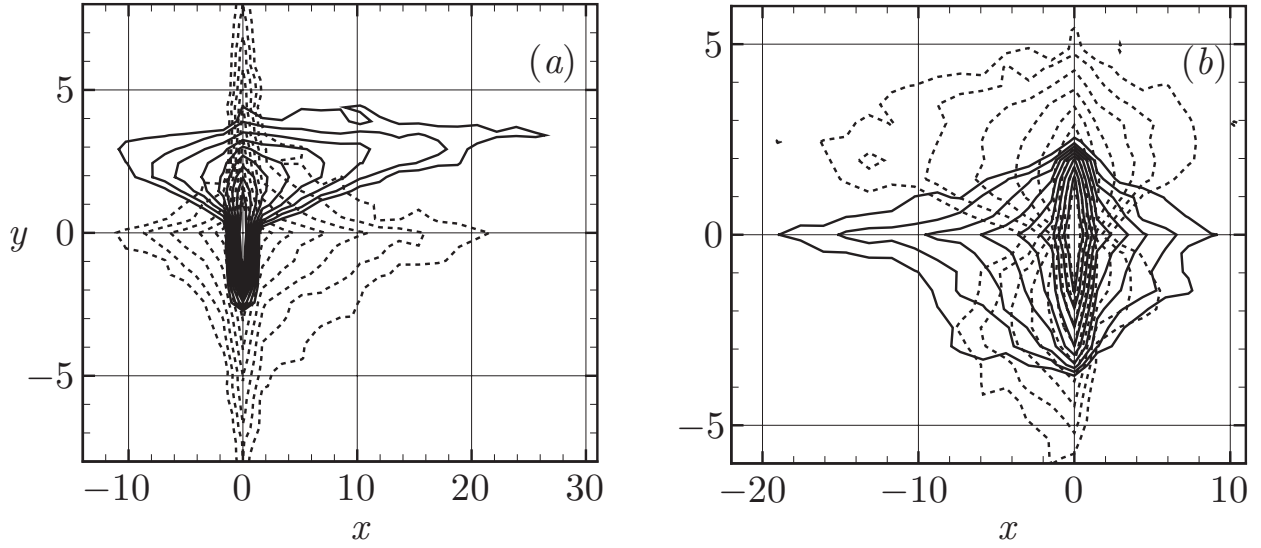


Figure 1: Schematic of the voltage divider inside the PMU.

can maintain connection at up to 250 RPM. They consist of six power rings that can each carry up to 50 A, and 54 additional signal rings that carry no more than 10 A, and are meant for low-voltage sensor signals (see section ???).

C.1.5 Rotating Frame Wiring

C.2 Plumbing

C.2.1 Rooftop Chiller

The rooftop chiller is an air cooled General Air recirculating water chiller. It has been installed on the roof, directly above our lab. Supply and return water lines have been hard-lined through the ceiling. From here, the water circuit is split into three lines, for each of the rooftop chillers three thermal loads. These loads are: the lab chiller, the magnet power supply, and the magnet itself. Each of these thermal loads requires at least 3 GPM of recirculating cool water, which is easily met by the rooftop chillers internal pump, and monitored by mechanical flowmeters. The returning, warmer water is cooled by a compressor, releasing RoMags residual heat to the atmosphere. When all three components are at maximum power, we should be generating less than 20 kW of excess heat. This is roughly the equivalent of an idling automobile.

C.2.2 Laboratory Chiller

Water is forced into the cooling block by a CP-75 pump in our Thermo NESLAB HX300 precision chiller, hereon called the lab chiller. The lab chiller maintains a reservoir of fluid (we use water) at a thermostated

temperature to within 0.1C.

C.2.3 Rotary Union

As in the case of the heater power supply, here we have to deliver chilled water from a source in the lab frame to the cooling block, which resides in the rotating frame. In order to accomplish this, we utilize a fluid rotary union. We use a two-channel rotary union manufactured by Rotary Systems ??? IS THIS THE NEW ONE?.

C.2.4 The Heat Exchanger

The heat produced by our heating element flows up into and through the convection tank (see section ??), above which it must be removed. This is accomplished by a liquid cooled aluminum heat exchanger, which is referred to as the cooling block, and is shown in figure ??. The cooling block is a cylindrical block of aluminum(T6061) into which has been cut two double wound spiral flow channels. Water is forced into the block at the inlet pipe connection and flows through either the top (figure ??) or bottom (not shown) channel. Here, it spirals inward and clockwise until it reaches the center of the cooling block after which point it spirals back outward and counterclockwise. This double spiral flow path is devised such that as the water flows through the cooling block and heats up, the general pattern of temperature will be roughly uniform. This, together with a thin (3/16") copper bottom cover, allows us to treat the bottom surface of the cooling block as nearly isothermal. STILL TRUE??.

- The heat exchanger requires two of the following oring: Dash No. 277 and McMaster #:9452K376

C.2.5 Flushing the Rooftop Chiller

C.2.6 Filling and Draining the Heat Exchanger

C.2.7 Filling and Draining the Laboratory Chiller

C.3 Troubleshooting

D. Gastrointestinal System

The gastrointestinal system of RoMag refers to the convection tanks, and the storage, transport, and experimental implementation (convection tank filling) of the working fluids. Working fluids are those

whose behavior we examine within the convection tank. They include (but are not necessarily limited to) water, sucrose solution, and gallium.

D.1 Fluid Properties

The thermophysical properties of the working fluids are dependent on their temperature. The fluid properties of the three fluids, water, sucrose solution, and gallium, are described here as a function of temperature. The fluid properties needed for the measurements made in this study are density (ρ), thermal expansivity (α_T), viscosity (ν), thermal diffusivity (κ), thermal conductivity (k), and specific heat (C_P).

D.1.1 Fluid Properties of Water

The properties of water, in the units given above, are [Lide \[2000\]](#):

$$\rho[kgm^{-3}] = 999.8 + 0.1041T - 9.718 \times 10^{-3}T^2 + 5.184 \times 10^{-5}T^3, \quad (3)$$

$$\alpha_T[K^{-1}] = 6.82 \times 10^{-5} + 1.70 \times 10^{-5}T - 1.82 \times 10^{-7}T^2 + 1.05 \times 10^{-9}T^3, \quad (4)$$

$$\kappa[m^2s^{-1}] = 1.312 \times 10^{-7} + 6.972 \times 10^{-10}T + 5.631 \times 10^{-12}T^2 + 2.633 \times 10^{-14}T^3, \quad (5)$$

$$k[Wm^{-1}K^{-1}] = 0.5529 + 2.662 \times 10^{-3}T - 2.374 \times 10^{-5}T^2 + 1.108 \times 10^{-7}T^3, \quad (6)$$

$$C_p = \frac{k}{\rho\kappa}, \quad (7)$$

where T is the temperature of the water in $^{\circ}\text{C}$.

D.1.2 Fluid Properties of Sucrose Solution

D.1.3 Fluid Properties of Gallium

The properties for gallium are not well constrained, especially the viscosity. In order for comparison to previous studies we use the following properties used in [King and Aurnou \[2013, 2015\]](#), [Bertin et al. \[2017\]](#), [Grannan et al. \[2017a,b\]](#):

$$\alpha_T[K^{-1}] = 1.25 \times 10^{-4}, \quad (8)$$

$$\rho[kgm^{-3}] = \rho_{mp}(1 - \alpha_T(T - T_{mp})), \quad (9)$$

$$C_p[Jkg^{-1}K^{-1}] = 397.6, \quad (10)$$

$$k[Wm^{-1}K^{-1}] = 31.3, \quad (11)$$

$$\kappa[m^2/s] = \frac{k}{\rho C_p}, \quad (12)$$

$$\mu = \nu\rho = \mu_o \exp\left(\frac{E_a}{RT_{ab}}\right). \quad (13)$$

Note that for the equation of density in (9) the density of the gallium at the melting point, $\rho_{mp}[kgm^{-3}] = 6.09 \times 10^3$ and the melting point temperature is $T_{mp}[^{\circ}C] = 29.8$. For the dynamic viscosity in (13), the reference dynamic viscosity is $\mu_o[Pa\ s] = 4.359 \times 10^{-4}$ and $E_a[Jmol^{-1}] = 4000$ are constants specific to gallium. The gas constant is given by $R[JK^{-1}mol^{-1}] = 8.3144$ and $T_{ab}[K]$ is the absolute temperature of the gallium in Kelvin.

D.2 The Tank

The convection tank is the belly of the experiment. The convection tank sits atop the pedestal in what we call ‘the stack’. The stack is essentially everything above the pedestal that co-rotates. Figure ?? shows a schematic of stack components. Just above the top of the pedestal is a separate stainless steel platform with three leveling screws between it and the pedestal, such that the tank can be leveled independently of RoMags frame. Above this platform sits our bottom insulator, a simple right cylinder constructed from CS85, an insulating material with thermal conductivity $k = 0.31[Wm^{-1}K^{-1}]$ and has an upper operating temperature limit of 1000 $^{\circ}C$. Above the bottom thermal block is the sidewall, and above that is the top thermal block. Together, these three components make up the convection tank, which contains the working fluid. Above the convection tank sits the cooling block (discussed in section ???). On top of the the cooling block is the expansion tank, discussed below, and several layers of closed foam insulation to minimize thermal communication with the environment. The stack is mechanically secured by eight stainless steel rods that are threaded into the bottom platform and tightened from above the cooling block with stainless steel nuts and washers WHAT SIZE???

The convection tank is comprised of top and bottom caps, called thermal blocks, into which fits a cylindrical sidewall.

D.2.1 Cylindrical Sidewalls

The sidewall is essentially a piece of 20 cm diameter tubing, cut to a variety of different heights. We have three bottom thermal blocks, four top thermal blocks, and about twenty different sidewalls.

The sidewalls are cut to different heights so that we can change the fundamental length scale of the system, and therefore have access to different (scale-dependent) parameter ranges. For example, the Rayleigh and Ekman numbers are dependent on the length scale to the third and second power, respectively. Changing the tank height is therefore our most effective method of spanning large ranges of these parameters. Several different materials are also used in sidewall construction. Typically, we use clear polycarbonate tubing for water experiments that allow us to see into the tank, which is important for tank filling procedures and experimental flow visualization. In gallium, an opaque fluid, we use instead stainless steel sidewalls, with which we can reach higher temperatures, as the plastic sidewalls will begin to deform near 60C and will melt at temperatures above 100C.

Another reason for using sidewalls of different material for the different working fluids is due to the thermal conductivity. We would like to treat the sidewall as a perfect insulator. This is important for two reasons: first, heat escaping outward from the sidewalls gives us a height-dependent Nusselt number, which generates a number of dynamical and technical concerns; second, heat traveling upward through the sidewall should be negligible relative to that transferred by convection. The former concern is ameliorated by adding additional layers of closed-foam or fibrous insulation batting outside the tank (non-toxic Insulfrax insulation is used for high temperature applications as a safe alternative to fiberglass). The latter issue is problematic when undertaking low Nu experiments in water. The ratio of heat passed vertically through the sidewall $Q_{sidewall}$ to that through the fluid Q_{fluid} is:

$$\frac{Q_{sidewall}}{Q_{fluid}} = \frac{k_{sidewall}A_{sidewall}}{Nuk_{fluid}A_{fluid}} \quad (14)$$

where k is thermal conductivity of each medium, A is the area of a horizontal cross-section of each component, and Nu is the Nusselt number. Note that $k_{fluid}Nu$ can be treated as an effective thermal conductivity of a convecting medium. Using stainless steel, $k_{sidewall} = 16Wm^{-1}K^{-1}$, and water, $k_{H_2O} = 0.6Wm^{-1}K^{-1}$, as well as $A_{sidewall} = \pi(4''^2 - (4 - 1/8)''^2) = 3.1''^2$ for the 1/8 thick sidewalls, and $A_{fluid} =$

$\pi((4 - 1/8)^2) = 47.2^2$ for the fluid layer, the heat ratio is

$$\frac{Q_{sidewall}}{Q_{H_2O}} = 1.75Nu^{-1}, \quad (15)$$

between stainless steel sidewalls and water. This is a Nu dependent effect, and will be more significant at lower Nu . When seeking Nu scaling laws, the lower Ra data will have an anomalously low Nu (relative to the case of insulating sidewalls). We would then measure an α that is too low. Therefore, stainless steel sidewalls should not be used for convection in water. In gallium, however, $k_{fluid} = 31 Wm^{-1}K^{-1}$, and so the stainless sidewalls will have a much weaker effect:

$$\frac{Q_{sidewall}}{Q_{Ga}} = 0.034Nu^{-1}, \quad (16)$$

The thermal blocks, top and bottom, make up the other two components of the convection tank. The thermal blocks have smooth, flat surfaces that interface with the working fluid. Six holes are drilled radially inward from the sides of each thermal block for temperature probes. These holes, seen in figure 16 are equally spaced in azimuth, and are located just 3 mm from the fluid surface. The bottom thermal block has a filling port through which we fill and empty the convection tank. The top thermal blocks have two additional ports, one for tank overflow and decompression during filling and draining procedures, and another to be connected to an expansion tank.

D.2.2 The Expansion Tank

The expansion tank is a stainless steel tank that is attached to the top of the cooling block and permanently open to overflow from the convection tank. The expansion tank gets its name from its purpose: it serves as a reservoir for excess working fluid resulting from thermal expansion during convection experiments. This allows the convection tank to be effectively open to atmosphere so that pressurization issues don't arise, and assures that the convection tank, once full, will remain so despite thermal expansion and contraction of the working fluid as mean temperatures fluctuate.

- The top and bottom thermal blocks each have the following oring: Dash No. 171 and McMaster #9452K329

D.2.3 The Top and Bottom Thermal Blocks

The top thermal block also houses internal temperature and velocity sensors. As in the selection of sidewall material, the design of the top and bottom thermal blocks also holds conductivity ratios as a main concern. A basic assumption of Rayleigh-Bénard convection is that the top and bottom fluid boundaries are isothermal. In real experiments, the bounding surfaces have finite conductivity, $k_{surface}$, which allows temperature variations to form. The Biot number, Bi , characterizes the ‘isothermality of the boundary in a heat transfer problem by comparing the temperature drop in the boundary to that of the interior (or, more accurately, compares the total effective conductance of the layers, which is equivalent to temperature drop assuming conservation of vertical heat flux on horizontal planes). Low Bi systems will have smaller thermal variations in the boundaries than in the interior. The Biot number is defined as

$$Bi = h \frac{D_{surface}}{k_{surface}}, \quad (17)$$

where h is the overall heat transfer coefficient, $D_{surface}$ is the boundary thickness, and $k_{surface}$ is the boundarys thermal conductivity. Thus, for convection,

$$Bi = \frac{k_{fluid}}{k_{surface}} \frac{D_{surface}}{D_{fluid}} Nu. \quad (18)$$

We assume that our heater and cooling block represent isothermal surfaces, and the bounding surfaces in question are then our top and bottom thermal blocks. We also assume that $Bi \leq 0.1$ corresponds to negligible temperature gradients in the boundary. Above this value, convective behavior can be influenced significant thermal heterogeneity in the boundaries. It can be seen in (18) that Bi will be largest for tall tanks of gallium. The goal of our convection tank design is to maximize our available Nu under the constraint that $Bi \leq 0.1$ for convection in liquid gallium. There are two ways to do this according to (18): maximize the boundaries thermal conductivity, and minimize the boundaries thickness.

Thus we have designed and constructed thermal blocks from copper ($k_{copper} = 390 W m^{-1} K^{-1}$), and we have made them as thin as possible. For the bottom thermal block, the limiting factor in how thin the block can be made is in the filling port, which becomes too small for reasonable fill times below 1/8” NPT (national pipe threading). We designed the block to be only 0.6 (0.015 m) thick, which allows Nusselt numbers as high as 16.4 with $Bi \leq 0.1$ for a 20 cm tank of gallium.

The top thermal block is a bit more tricky. The need for a top thermal block to house temperature and velocity sensors brought us to design two separate top blocks, one with portholes for sensors and another, thinner block without. The thinner block has thickness 0.52" (0.013 m), made possible by using smaller 1/16" NPT filling ports. This together with the 3/16" thick cover on the cooling block allows us to reach $Nu \leq 13.9$ for $Bi \leq 0.1$.

The second top thermal block must house the diagnostic sensors, and so must be both considerably thicker, and must have non-negligible void space for the probes, further reducing its effective conductance. With this block, whose design is shown in figure ?? and has total thickness 1.85" (0.047 m), we can reach $Nu \leq 5.7$ for $Bi \leq 0.1$.

Another difficulty faced in thermal block design for use with gallium is due to the corrosive nature of the liquid metal. Gallium reacts with copper. Despite this fact, all protective coatings that were described in [King \[2009\]](#) have since been removed. Convection experiments in water require less restrictive thermal block design. Here, we use any combination of the copper blocks described above, and four more made from aluminum ($T6061$, $k_{aluminum} = 167 W m^{-1} K^{-1}$).

D.2.4 Internal Thermistor Holders

Up to eight Delrin thermistors holders can be inserted into the convection tank through the top thermal block. The thermistor holders are held in the thermal block with three screws. The internal thermistor is held in the thermistor with a set screw. The thermistor and thermistor holder use three orings for sealing.

- A very small ring is placed around the internal thermistor and is compressed when the internal thermistor is inserted into the thermistor holder. Oring Dash No. 101 McMaster #:9452K111
- Two orings are placed around the thin shaft of either the thermistor holder or the the doppler probe. The round oring goes on first and the x shaped oring goes on second. Round oring: Dash No. 903, McMaster #:9751K113, x oring: Dash No. 010, McMaster #:90025K133

The planform arrangement of possible thermistor locations is shown in the top thermal block drawing in figure 20.

D.3 Assembling the Stack

D.4 Troubleshooting

E. Water Storage, Degassing, and Filling

Water storage is somewhat simple. We use tap water for our experiments, as water in its purer (deionized and distilled) forms is more corrosive. We keep a holding tank full of water at a high point in the lab. This tank is loosely sealed, to allow the water to degas while preventing significant evaporation. Degassing water is important because otherwise the fluid will release gas when heated in the convection tank, and this will generate bubble formation at the top of the convection tank. In Rayleigh-Bénard convection, the tanks top and bottom surfaces must be completely wetted???. The formation of bubbles, or a less than completely filled tank forms an unintentional and effective obstacle for heat transfer. Much of the convection tank filling process is developed to ensure proper wetting of the top boundary.

The convection tank is filled with water by way of gravitational pressure and a system of rubber tubing and plastic quick-disconnect tube fittings and valves. Prior to filling, the tank is tilted so that the overflow port is near the high-point. This forces the air in the tank to be forced out of the system to avoid bubble formation. Alternatively, bubble formation can be avoided by filling a tank that has been evacuated. Tank evacuation is accomplished using a modified bike tire pump. By reversing the plunger and check valve of a bike pump, I apply negative pressure to the top of the expansion tank. This is especially effective when the convection tank is partially full, so that any air trapped in the filling tubes will be evacuated as well. In order to maintain the vacuum, a well sealed experiment is required. A pressure valve is affixed to the top of the expansion tank to avoid building positive pressure in the closed system. If the water has not been completely degassed, introducing it to less-than-atmospheric pressure will force further degassing. This is counter-productive in the quest for perfect wetting, and so tank evacuation is most often used in the gallium filling procedure.

F. Gallium Storage, Cleaning, and Filling

F.1 Storage

F.2 Gallium Cleaning

The major parts of the gallium cleaning system are the fumehood where the system is located, the stainless steel storage tank where the gallium is stored, the peristaltic pump is used to push the gallium around, the white cleaning tank where the cleaning takes place, and the tubing that connects everything together. The following information assumes that you approach a cold fumehood.

- Make sure the piping system is put together in the same manner as it will be for cleaning.
- Several days before beginning the gallium cleaning process start the monitoring system to measure temperatures. Plug the band heater and heating fan into the 3 phase outlet on the right side of the front of the fumehood.
- It is necessary to keep the fumehood at 40C for several days in order to ensure that the gallium is completely melted throughout the entire system. Thus one should make sure that step one is done so that melted gallium does not fall out unnecessarily.
- It is then necessary to flush the plumbing system in order to ensure there are no blockages. This is performed by disconnecting the plumbing system at various points and pumping Argon gas through for a few minutes. Take care in disconnecting the plumbing system to avoid losing gallium unnecessarily.

DETAILS

- Once the pumping system has been cleared you begin pumping gallium through the system without actually cleaning it. make sure the valve coming out the bottom of the storage tank is open, the peristaltic pump is clamped down on both tubes. make sure the valve going into the white gallium cleaning tank is in the down position, and the valve going into the top of the storage tank is open. Check for leaks and address any. The tall pipe going to the top of the storage container may need to be disconnected and primed.
- Turn on the peristaltic pump making sure the pumps are rotating counterclockwise and the speed is around 12-15.

- To determine the strength of the pumping you have to look at the level of the gallium in the cleaning tank. The strength of the pumping is controlled by the two black nobs on the top of the peristaltic pump. These knobs can be adjusted and you can watch the response of the level of the gallium in the tank. Roughly the knob is set to 4ish on the front knob controlling the inflow into the cleaning tank and 5ish for the outflow leaving the cleaning container. While there seems to be a strong sensitivity in the knob settings, it is likely that the inflow should be less than the outflow because the inflow gets a kick from the pressure in the gallium storage tank while the outflow is pushing fluid into the top of the storage tank.
- For cleaning the gallium, the pumping system must be turned on as described above. In addition the heat pad and stirrer beneath the cleaning tank can be turned to 40C and halfway on the stirring. The clear container above the white cleaning container is filled with one part HCL and 9 parts water. By opening the valve on the clear container add about a 0.5cm thick layer of acid solution. Pump the gallium through the system and the duration is variable from 30 minutes to several hours.
- Keep an eye on the fluid level in the cleaning container as it can change and the knobs controlling the flow are quite sensitive and still need to be determined.

F.3 Before the Gallium Transfer

Several steps are necessary for filling the tank.

F.3.1 Room

- Turn up the temperature of the room to the highest possible level the night before so that the room is warm to help facilitate the gallium transfer

F.3.2 Fumehood

- Make sure that the gallium has been cleaned.
-

F.3.3 Transfer Hose

- Make sure the transfer hose has been warmed up and cleared using Argon gas.

- Make sure that the transfer hose has been primed for pumping gallium through it such that it is filled with gallium and a majority of the bubbles are removed. The setting for the speed of the pump can be high between 15-20

F.3.4 Experimental Stack

- Put the entire stack together as it will be when filled with gallium with the modifications that the top thermal lid outlet not going to the expansion tank is connected to a hose and then a container to catch excess gallium. This modification may be optional as discussed below. Also use plastic wrap to cover up the electronics in the central part of the pedestal. Be sure to cover thermocouple connectors, thermistor connectors etc. in this region.
- Warm the entire stack with the heater between 20-50W and lab chiller at 35C starting several hours before the filling. By the time of the filling the stack should be above 35C to accept the liquid gallium. The entire assembly should be hot to the touch including the metal valves attached to the inlet and outlets.
- In an effort to prevent bubbles forming, the stack needs to be tilted at an angle so that the outlet not going to the expansion is the highest point. It is questionable whether this step is necessary but we may be helpful to determine with certainty where the gallium is especially when the opaque stainless steel cylinder is used. Note that the location of the gallium can also be determined by the internal thermistors sitting at multiple depths inside the fluid layer.
- Flush the experimental cylinder and expansion tank with Argon gas for around 10 minutes.

F.4 During the Filling

- The transfer hose is plugged from the fumehood to the inlet on the lower lid. Its weight needs to be well supported.
- The pump should be set for a slow fill with the speed of the peristaltic pumping to be around 3-5.
- Monitor thermistors and perhaps thermocouples to track the level of the gallium.
- During the filling, once gallium has reached the high point and is flowing out of the outlet into a container for 1-2 minutes, the peristaltic pump is stopped and the the stack is then tilted so that the

outlet going to the expansion tank is now the highest point.

- Use the thermistors and thermocouples in the expansion tank, and also visual inspection where possible to determine the level of the gallium in the expansion tank.
- Once the gallium has filled the expansion tank halfway shut of the pump.
- Monitor the stack for leaks.

F.5 Emptying the Tank

F.6 Troubleshooting

G. DDC Alarms and Safety Controls

G.1 Alarm Control

G.2 Alarm Definitions

Name:Suffix	Description	Formula	Location	Address
SPINLAB.ALARM.ENABLE	Alarm Enable Cmd	-	Lab	-Virtual-
SPINLAB.HX300.CHLR.PRF	Lab Chiller Proof	-	Lab	0 00 16
SPINLAB.HX300.CHLR.SS	Lab Chiller State	-	Lab	-Virtual-
SPINLAB.HX300.LEVEL.ALM	Lab Chiller Water Level Alarm	-	Lab	0 00 11
SPINLAB.HX300.TEMP.ALM	Lab Chiller Temp. Alarm	-	Lab	0 00 12
SPINLAB.ROMAG.GaXFER	Gallium Transfer Condition	-	Lab	-Virtual-
SPINLAB.ROMAG.HORN	Horn Alarm	-	Control Box	0 00 20
SPINLAB.ROMAG.IR	IR Temp Reading	-	Ceiling above Romag	0 00 05
SPINLAB.ROMAG.MODE	System Mode	-	Control Box	0 00 07
SPINLAB.ROMAG.RMRH	Room Relative Humidity	-	Control Box Left Side	0 00 06
SPINLAB.ROMAG.RMT	Room Temp	-	Control Box Left Side	0 00 05
SPINLAB.ROMAG.TCu	Lower Thermal Block Temp	-	RoMag	0 00 15
SPINLAB.ROMAG.Tin	Magnet Inlet Temp	-	Magnet	0 00 13
SPINLAB.ROMAG.Tout	Manget Outlet Temp	-	Magnet	0 00 14
SPINLAB.ROMAG.Td	Magnet Temp Drop	$T_{out} - T_{in}$	Magnet	-Virtual-
SPINLAB.ROMAG.Trm	Average Differential Temp	$(T_{out} + T_{in})/2 - RMT$	-	-Virtual-
SPINLAB.ROMAG.WATER	Floor waterbug	-	Floor under RoMag	0 00 02
SPINLAB.ROMAG.WET	Pan Water Sensor 1	-	RoMag Pan	0 00 09
SPINLAB.ROMAG.WET2	Pan Water Sensor 2	-	RoMag Pan	-Virtual-
SPINLAB.ROOF.CHLR.PRF	Roof Chiller Proof	-	Roof	0 00 01
SPINLAB.ROOF.CHLR.SS	Roof Chiller State	-	Roof	-Virtual-

Table 1: Table of alarm definitions and locations.

G.3 Alarm Priorities

To prevent overheating in some instances or freezing of Gallium in other instances, different temperature values and ranges are assigned one of three different priorities

G.3.1 P1: “Highest Priority”

The first level of security where the Spinlab group, David Riley, Gary Glesener, and Kathleen Micham are sent emails and texts.

G.3.2 P2: “Medium Priority”

The second level of security where the Spinlab group gets emails and texts.

G.3.3 P3: “Low Priority”

The third level of security where the Spinlab group gets emails and texts.

Mode 1: SPINLAB_ROMAG.MODE: Standby									
Used for non-operation, water transfer, and water sleep mode									
Roof Chiller Off	Lab Chiller Off	Argantix Off	Magnet Off	Servo Off	Waterbug On	Wet 1&2 On	Thermal Block P3: $5C > TCu > 60C$ P2: $2C > TCu > 70C$ P1: $0C > TCu > 80C$	IR Sensor $IR > 60C$ $IR > 70C$ $IR > 80C$	Magnet Temp $Td > 10C$ or $Trm > 10C$ $Td > 20C$ or $Trm > 20C$ $Td > 30C$ or $Trm > 30C$
Mode 2.1: SPINLAB_ROMAG.MODE: H₂OConv									
Used for water RBC									
Roof Chiller On	Lab Chiller On	Argantix On	Magnet Off	Servo Off	Waterbug On	Wet 1&2 On	Thermal Block P3: $5C > TCu > 75C$ P2: $0C > TCu > 85C$ P1: $-5C > TCu > 90C$	IR Sensor $5C > IR > 75C$ $0C > IR > 85C$ $-5C > IR > 90C$	Magnet Temp $Td > 10C$ or $Trm > 10C$ $Td > 20C$ or $Trm > 20C$ $Td > 30C$ or $Trm > 30C$
Mode 2.2: SPINLAB_ROMAG.MODE: H₂OConv									
Used rotating convection in water									
Roof Chiller On	Lab Chiller On	Argantix On	Magnet Off	Servo On	Waterbug On	Wet 1&2 On	Thermal Block P3: $5C > TCu > 75C$ P2: $0C > TCu > 85C$ P1: $-5C > TCu > 90C$	IR Sensor $5C > IR > 75C$ $0C > IR > 85C$ $-5C > IR > 90C$	Magnet Temp $Td > 10C$ or $Trm > 10C$ $Td > 20C$ or $Trm > 20C$ $Td > 30C$ or $Trm > 30C$
Mode 3: SPINLAB_ROMAG.MODE: GaXfer									
Used for transferring the Gallium from the fumehood									
Roof Chiller On	Lab Chiller On	Argantix On	Magnet Off	Servo Off	Waterbug On	Wet 1&2 On	Thermal Block P3: $32C > TCu > 75C$ P2: $31C > TCu > 85C$ P1: $30C > TCu > 90C$	IR Sensor Tests Needed Tests Needed Tests Needed	Magnet Temp $Td > 10C$ or $Trm > 10C$ $Td > 20C$ or $Trm > 20C$ $Td > 30C$ or $Trm > 30C$
Mode 4: SPINLAB_ROMAG.MODE: GaSleep									
Used for non-operation of Gallium filled container									
Roof Chiller On	Lab Chiller On	Argantix On	Magnet Off	Servo Off	Waterbug On	Wet 1&2 On	Thermal Block P3: $32C > TCu > 75C$ P2: $31C > TCu > 85C$ P1: $30C > TCu > 90C$	IR Sensor Tests Needed Tests Needed Tests Needed	Magnet Temp $Td > 10C$ or $Trm > 10C$ $Td > 20C$ or $Trm > 20C$ $Td > 30C$ or $Trm > 30C$
Mode 5.1: SPINLAB_ROMAG.MODE: GaConv									
Used for RBC in Gallium									
Roof Chiller On	Lab Chiller On	Argantix On	Magnet Off	Servo Off	Waterbug On	Wet 1&2 On	Thermal Block P3: $32C > TCu > 75C$ P2: $31C > TCu > 85C$ P1: $30C > TCu > 90C$	IR Sensor $32C > IR > 75C$ $31C > IR > 85C$ $30C > IR > 90C$	Magnet Temp $Td > 10C$ or $Trm > 10C$ $Td > 20C$ or $Trm > 20C$ $Td > 30C$ or $Trm > 30C$
Mode 5.2: SPINLAB_ROMAG.MODE: GaConv									
Used for rotating convection in Gallium									
Roof Chiller On	Lab Chiller On	Argantix On	Magnet Off	Servo On	Waterbug On	Wet 1&2 On	Thermal Block P3: $32C > TCu > 75C$ P2: $31C > TCu > 85C$ P1: $30C > TCu > 90C$	IR Sensor $32C > IR > 75C$ $31C > IR > 85C$ $30C > IR > 90C$	Magnet Temp $Td > 10C$ or $Trm > 10C$ $Td > 20C$ or $Trm > 20C$ $Td > 30C$ or $Trm > 30C$
Mode 6.1: SPINLAB_ROMAG.MODE: GaMagCon									
Used for magnetoconvection in Gallium									
Roof Chiller On	Lab Chiller On	Argantix On	Magnet On	Servo Off	Waterbug On	Wet 1&2 On	Thermal Block P3: $32C > TCu > 75C$ P2: $31C > TCu > 85C$ P1: $30C > TCu > 90C$	IR Sensor $32C > IR > 75C$ $31C > IR > 85C$ $30C > IR > 90C$	Magnet Temp $Td > 10C$ or $Trm > 10C$ $Td > 20C$ or $Trm > 20C$ $Td > 30C$ or $Trm > 30C$
Mode 6.2: SPINLAB_ROMAG.MODE: GaMagCon									
Used for rotating magnetoconvection in Gallium									
Roof Chiller On	Lab Chiller On	Argantix On	Magnet On	Servo On	Waterbug On	Wet 1&2 On	Thermal Block P3: $32C > TCu > 75C$ P2: $31C > TCu > 85C$ P1: $30C > TCu > 90C$	IR Sensor $32C > IR > 75C$ $31C > IR > 85C$ $30C > IR > 90C$	Magnet Temp $Td > 10C$ or $Trm > 10C$ $Td > 20C$ or $Trm > 20C$ $Td > 30C$ or $Trm > 30C$

Table 2: Table of alarm definitions and locations.

H. Nervous System

H.1 Labview Monitoring System: Front Panel

H.2 Labview Monitoring System: Back Panel

H.2.1 Gathering Channel Information

H.2.2 Displaying Data

H.2.3 Calculating Dimensional Quantities

H.2.4 Calculating Non-Dimensional Quantities

H.2.5 Sending Monitor Emails

H.2.6 Saving Data

H.3 Labview Alarms and Notifications

H.4 Labview Monitoring and Alarms Troubleshooting

To control Romag, a Labview program is used to issue VISA commands that are sent to Omega voltage supplies. Currently only two Omegas are used to control the heated and the chiller set temperatures.

H.5 Heat Pad Control

H.6 Lab Chiller Control

H.7 Roof Chiller Control

H.8 Rotation Control

H.9 Magnet Control

H.9.1 Raising and Lowering the Magnet

H.9.2 Changing the Magnetic Field

H.10 Lab Chiller Flow Rate Control

H.11 Controls Troubleshooting

I. Measurements

I.1 Measuring Rotation

We do not currently measure the rotation rate. The rotation rate is manually input into the labview program by the user.

I.2 Measuring Magnetic Field Data

We do not currently measure the magnetic field with hall probes. The amperage is manually input into the labview program by the user.

I.2.1 Hall Probes

I.2.2 Magnet Current Sensor

I.3 Measuring Thermal Data

The SCXI 1300 excitation module sends a known (small) current through each thermistor, and measures the resulting voltage drop, which can be converted into a resistivity. This resistivity measurement is converted

into measurements of temperature by the Labview software on the PXI box by using the coefficients determined for each thermistor. Thus, the data acquisition software outputs measurements of temperature for each thermistor.

I.3.1 Thermistors

Temperature measurements are made using thirty-eight custom made GE Thermometrics sheath thermistors. Thermistors use resistance elements (here, ceramic) whose resistivity is temperature dependent. A third-order approximation of the relationship between temperature and resistivity is given by the Steinhart-Hart equation:

$$\frac{1}{T} = a + b\ln(R) + c\ln^3(R) \quad (19)$$

where R is the resistivity of the thermistor. A thermistor's resistivity can be measured by passing a small known current through it and measuring the resulting voltage drop. This equation can be used to solve for temperature as a function of resistivity, provided the coefficients a , b , and c are known. These coefficients are particular to each thermistor, and can be solved for by measuring the resistivity of each thermistor at three known temperatures. This is accomplished by immersing all of the thermistors in the thermostated reservoir of a precision chiller. I measure the resistivities of each thermistor for 10-15 minutes at 10 Hz. This is done for each of five temperatures $T1$, $T2$, $T3$, $T4$, and $T5$ spread across an expected range of RoMag operating temperatures. The resistivity measurements are averaged in time to get three values $R1(n)$, $R2(n)$, $R3(n)$, $R4(n)$, and $R5(n)$ for each of n thermistors, corresponding to the three different temperatures. The coefficients for each thermistor (a , b , and c) can then be solved for in MATLAB using the Steinhart-Hart equation.

The SCXI 1300 excitation module sends a known (small) current through each thermistor, and measures the resulting voltage drop, which can be converted into a resistivity. This resistivity measurement is converted into measurements of temperature by the Labview software on the PXI box by using the coefficients determined for each thermistor. Thus, the data acquisition software outputs measurements of temperature for each thermistor.

Thermistor calibrations are tested by again immersing the thermistors in an isothermal bath, this time at a temperature different from $T1$, $T2$, and $T3$. Another, more comprehensive test is done before running experiments. When the convection tank is full and insulated, the heater is turned off and the chiller is set to a temperature near ambient. After sufficient time, the system should thermally equilibrate and the

thermistors should all read the same temperature. These tests show that my calibrations are good to better than ± 0.01 K. The quality of the insulation can be tested by fixing the cooling block temperature higher or lower than ambient. If the tank is perfectly insulated, one should again observe constant temperatures throughout the stack after the system has equilibrated.

At present, the most useful measurements made in RoMag are the Nusselt and Rayleigh numbers. These parameters require essentially two dynamic measurements: mean temperature drop; and total heat flux. The mean temperature drop is calculated as the difference between the average bottom and top thermistor measurements. The heat flux measurement is made in two ways: by using the electrical power supplied to the heater (discussed above), and by measuring the temperature change and the heat losses through the sidewall.

I.3.2 Sidewall Heat Losses

See [Cheng \[2015\]](#) These thermistors have varying length, and can then be placed within the tank at varying vertical locations.. Typically, the central thermistor is placed at the very center of the tank, for comparison with other thermal turbulence studies. These thermistors have stainless steel sheaths of only 0.9 mm thick. This allows measurements high frequency temperature statistics within the fluid.

I.3.3 Thermocouples

I.4 Labview Acquisition

J. Acquiring Velocity Data

J.0.1 Doppler Velocimetry

Visualization techniques for fluid dynamics experiments abound. However, liquid metals are opaque, a quality that renders almost all visual diagnostics ineffective. Flow measurements can be made in gallium using the relatively new acoustic Doppler velocimetry technique. Although results from Doppler measurements are not shown in the results presented in this document, a description of the development of this experimental technique is included here for completeness.

At the heart of acoustic velocimetry is the piezoelectric transducer, which is basically a small-scale speaker/microphone. Probes containing piezoelectrics send high frequency sonar pulses into the fluid, and

listen for backscattered acoustic signals. Assuming we know the speed of sound in the fluid, the time delay between the initial chirp and the incident backscatter gives the position of the fluid parcel in question. The probes sounding is repeated at high frequency. Moving fluid parcels will scatter energy that is well correlated with that from the last iteration. Maximizing auto-correlations in space shows how far the parcel has moved since the last chirp. This permits measurement of velocity as a function of time, along a one-dimensional beam. The velocity measured is also one-dimensional, co-linear with the orientation of the acoustic beam. We use a Met-flow Ultrasonic Velocity Profiler (UVP) Duo MX Doppler system, with custom made probes operating at 2, 4, and 8 MHz. The Doppler signals are acquired in the rotating frame using the UVP Duo MX (called the Doppler box in figure ??). The Doppler system is controlled by a PC in the lab frame through an ethernet line. I found that the most reliable method of ethernet communication between lab and rotating frames to be through the power slip-rings, using a commercially available powerline ethernet adaptor (NETGEAR XEB1004).

Acoustic energy is reflected by imperfections in the medium that present a local impedance to the sound wave. In gallium, these imperfections are naturally occurring oxides. In water, the scattering particles must be seeded in the fluid. We use polystyrene microspheres, shown in figure ??. The particles are typically between 50 and 100 μm in diameter, and have density 1.050gcm^{-3} . It is important that the seed particles are neutrally buoyant in the fluid medium. For this reason, we add sugar to water to match the solutions density to that of the seed particles. Empirically, we find we need 144.4 g of sugar per L of water for solution $\rho_{\text{saturation}} = 1.050\text{gcm}^{-3}$ (corresponding to 14.4 Brix).

Stokes Law describes how fast spherical bodies fall through viscous fluids, assuming laminar flow (?:

$$v = \frac{1}{18} \left[\frac{(\rho_s - \rho_f)gd^2}{\mu} \right] \quad (20)$$

where v is settling velocity, ρ_s is the density of the solid sphere, ρ_f is the fluid density, g is gravitational acceleration, d is the spheres diameter, and μ is the the dynamic fluid viscosity, $\mu = \nu\rho_f$, where ν is the kinematic viscosity. Thus,

$$v = \frac{1}{18} \left[\frac{\delta_\rho gd^2}{\nu} \right] \quad (21)$$

where δ_ρ is the density difference fraction $(\rho_s - \rho_f)/\rho_f$. The time it takes for the particles to fall from

suspension in the 5 cm tank can be estimated as

$$t_{\text{settle}} = \frac{0.05\text{m}}{v} = \frac{9.2}{\delta_\rho} \text{seconds} \quad (22)$$

So settling time is inversely proportional to the error in density matching sugar water to particle density. Thus, if the fractional density difference is ten percent, the particles will all settle out within a minute and a half. If the mismatch is one percent, it will take fifteen minutes. This relationship is shown in figure ???. A typical thermal equilibrium time for convection experiments is about three hours. In order to keep the seed particles in suspension for three hours in a laminar fluid, a density matching of better than one part in a thousand is required. Fortunately, the presence of turbulence in most of our convection runs will keep the microspheres adequately stirred for the duration of a typical experiment.

The Doppler probes are cylindrical (resembling crayons in shape and size), and are made from either Delrin (a plastic) or stainless steel (for high temperature applications). We situate our probes either pointing downward in one of the probe holes shown in figure 20, or pointing horizontally through the sidewall. The orientation of sidewall probes is shown in figure 23. Two basic probe orientations are possible: a radial profile, intersecting with the tanks center, and a cord profile, at angle of 42° from the radial direction. The probe holders are machined from stainless steel, and are affixed to the stainless steel sidewalls using a silver weld. Welded joints between probe holders and sidewalls are coated in acrylic nail polish to protect the silver from gallium corrosion.

Doppler velocimetry is tested by way of impulsive spin-up. Spin-up (or spin-down) refers to the transient adjustment of a fluid from one state of solid body rotation to another. The control parameters here are:

$$\text{Ekman number} = E = \frac{\nu}{2\Omega H^2} = \frac{\text{viscous}}{\text{Coriolis}}; \text{Rossby number} = \epsilon = \frac{\Omega_2 - \Omega_1}{\Omega} \quad (23)$$

where ν is the fluids kinematic viscosity, the length scale, H , is the cylinder height, Ω is the background rotation rate, and Ω_1 and Ω_2 are the initial and final rotation rates, respectively. Most often, Ω is set to be the larger of Ω_1 and Ω_2 (save for the early linear spin up work by Greenspan and Howard ??? who used $\Omega = \Omega_1$). The Ekman number is usually assumed to be small ($E \ll 1$), and the Rossby number will fall in the range $1 \geq \epsilon \geq -1$, (e.g. $\epsilon > 0$ for spin-up and $\epsilon = -1$ is spin-up from rest).

When the tank is impulsively spun-up, the fluid will, at first, remain in its initial solid body rotation state, now rotating past the probe at a rate of $\epsilon\Omega$. In the case of linear spin-up ($\epsilon \ll 1$), the solution for

the evolution of the azimuthal velocity is (Greenspan (???)):

$$u_\phi = -\epsilon\Omega r \exp(-2E^{1/2}\Omega t) \quad (24)$$

where t is time after the impulse.

We measure this spin-up process with our cord profile Doppler probe. Figure ?? shows the geometry of the cord profile. Doppler velocimetry, again, measures co-linear velocity, which corresponds to $\mathbf{u} \cdot \mathbf{x}$ in Figure ??. If we assume a solid body rotation flow structure $\mathbf{u}_{\text{sb}} = \Omega r \hat{\phi}$, our probe will ‘see’ $\mathbf{u}_{\text{sb}} \cdot \hat{\mathbf{x}} = \Omega r \cos \theta = \Omega r \frac{y}{r} = \Omega y$. So we expect to measure linear spin-up velocities that are constant along this chord profile.

Figure ?? shows instantaneous velocity data along the chord profile shortly after the impulse. The relatively constant velocity measurement as a function of distance from the probe verifies that the probes can ‘see to the other side of the tank. Figure ?? shows raw velocity data at four points spanning the chord profile along with the theoretical curve from equation ??. The agreement between the measurement and theory verifies the accuracy of the doppler velocimetry technique in sucrose solution, even for slow fluid velocities. Spin-up tests like these can be performed just prior to and just after taking data in a convecting fluid in order to verify the validity of the Doppler data.

K. Acquiring Flow Rate Data

L. Flow Visualization

NOT CURRENT???? Visualizations are acquired in water experiments by using a Watec 902H Ultimate video camera in the laboratory frame. The camera is connected to a laptop via an analog-to-digital converter, and is captured using BTV Pro software. Still images may be sampled from the video stream, examples of which are shown in figure ?? on page ??. The fluid is injected with a Kalliroscope solution, which contains small, flake-like particles that stay in suspension and tend to align with shear structures in the flow. They reflect light in such a way as to reveal instantaneous flow structures.

The convection tank is illuminated by way of a laser light sheet. This is a laser beam which has been sent through a cylindrical lens that spreads the light into a two-dimensional planar sheet. We orient the light sheet to shine vertically through the center of the tank. The Kalliroscope solution must be dilute

enough that the laser light reaches the far end of the tank, yet rich enough to provide sufficient contrast for imaging. More concentrated Kalliroscope solutions permit observations of fluid behavior just inside the sidewall, as seen in figure ??.

M. Running Cases

Here, I outline a typical sequence of operations for running convection experiments with RoMag, and the precise methodology by which the essential measurements presented in this document are made.

Starting with a fully assembled stack, the thermal data acquisition system is initiated so the fluid can be monitored. The tank is filled with the working fluid (see section ???) and insulated. Once the tank is full and insulated, the heating system is initiated by activating the roof chiller, lab chiller, and heat power supply. These must be activated and verified in this order, so heat is not trapped anywhere in the circulatory system (e.g., figure ??). A rotation rate is chosen to achieve the desired Ekman number based on the tank size in use. Rotation is slowly ramped up (25 RPM/second) to this desired rate using the servo control software (section ???). Solid body rotation should be achieved within several minutes (e.g., figure ??).

Next, a heat power is chosen in order to reach a desired flux Rayleigh number. The flux Rayleigh number is defined as:

$$Ra_f = RaNu = \frac{\alpha_T g H^4 q}{\rho C_p \kappa^2 \nu}, \quad (25)$$

where q is the heat flux, which is the heat power per unit area. With RoMag, I control the heat flux, not the temperature drop across the fluid. I do not, then, fix the Rayleigh number, but rather the flux Rayleigh number. In order to approach a desired Rayleigh number with this device, the relationship between Nu and Ra must be known a priori. The lower limit on heat power is determined by our ability to measure small heat fluxes through the cooling block (see section ???). Below about 5W, the difference between the heat power measured through the cooling block begins to differ significantly from the input heat power. I do not report results for experiments with heat fluxes of less than 10W. The upper bound for heat power is either 5 kW, which is the maximum output of the power supply, or determined by the limit of our maximum allowable temperature drop, ΔT . Our cooling block can be fixed to be no colder than about 5°C (in order to avoid freezing issues in the lab chiller). As ΔT increases, so does the peak temperature of the system. We limit the maximum temperature based on the weakest thermal component. For example,

polycarbonate begins to lose structural integrity above about 60°C. The maximum heat power is then dependent on the maximum ΔT , which is dependent on the materials present and the convecting fluids ability to transfer the heat upward.

Once a heat power value is chosen (typically, I start at the lowest value), the current is delivered to the heater. The response of the system is monitored thermally using the Labview software. Typically, the system takes approximately three hours to equilibrate. I consider the system thermally equilibrated when no trend is observed on any thermistor over a time period of 30 minutes. Once the system has equilibrated, I begin recording data at a typical rate of 10 Hz for about an hour. Once recording is finish, I change the heat power and wait for the system to re-equilibrate. Typically, I step logarithmically from the lowest to highest heating value so that I acquire approximately 15 Nu Ra cases for each Ekman number in each tank. Once these are acquired, I switch the rotation rate and again step through several heat power points. Convection cases are occasionally duplicated to verify repeatability. Once all desired Ekman numbers are acquired, I shut down the device, beginning with the servomotor, then the heater, followed by the lab chiller, rooftop chiller, and data acquisition system. I remove the insulation, drain the tank, and disassemble the stack. I then rebuild the stack with a sidewall of a different height, and repeat.

The data taken are as follows. Temperature time series are acquired from six thermistors in the bottom thermal block (figure ???), six thermistors in the top thermal block (figure 27b), up to eight or nine thermistors within the tank, and two thermistors measuring the input and output temperatures of the cooling block. Beyond this, several voltage time series measurements are acquired: from the current shunt and voltage divider to measure the power supplied to the heater; from the Proteus flowmeter to measure the flux of coolant through the cooling block; and from the servodrive to measure the rotation rate of the experiment. These data are stored in a text file by the Labview software on the PXI box for each convection case, and then transferred to an external hard drive. The data are processed using Matlab or Python.

Essentially, six separate quantities are discussed in this document that are calculated from these data for each convection case. They are the Prandtl, Ekman, Rayleigh and Nusselt numbers, and the temperature cross-covariance and central temperature variance measurements.

Four of these parameters are explicitly dependent on the physical properties of the fluid: the Prandtl, Ekman, Rayleigh, and Nusselt numbers. The fluid properties change with fluid temperature (section ???). In order to avoid large changes in the fluid properties, I try to keep the experiment near room temperature

($\sim 20^\circ\text{C}$). When I step up the power applied to the convection tank for each case, I also decrease the set point temperature of the lab chiller, and therefore decrease the temperature of the cooling block, in order to compensate for the growing temperature drop across the tank. This is an inexact tuning, but maintains nearly room temperature ($18\text{-}22^\circ\text{C}$) until the highest heat powers are reached. For most cases, then the fluid properties are fairly well-behaved. As the temperature drop across the fluid layer becomes larger than about 30°C , the mean temperature of the fluid will increase, changing (slightly) the properties of the fluid.

N. Post-Processing Data

N.1 Calculating Thermal Corrections

N.2 Calculating Sidewall Heat Losses

N.3 Calculating the Average Fluid Temperature

Using measurements from the top and bottom thermistors, the mean temperature of the fluid is calculated as

$$\langle T_{fluid} \rangle(t) = \frac{1}{12} \overline{\sum_{i=1}^6 T_i^{top}(t) \sum_{i=1}^6 T_i^{bot}(t)} \quad (26)$$

where the top and bottom thermal block temperature timeseries measurements are $T_i^{top}(t)$ and $T_i^{bot}(t)$, respectively, with $i = 1, \dots, 6$ corresponding to azimuthal location (see figure ??), and the overline represent averages in time. The fluid temperature calculation is shown in figure ???, before the measurement is time-averaged.

N.4 Calculating the Fluid Properties

Using this mean fluid temperature, the fluid properties for a given convection run are calculated using equations ???. This permits a calculation of the Prandtl number, $Pr = \nu/\kappa$ for each case.

N.5 Calculating the Ekman Number

In order to measure the Ekman number, $Ev = (2\Omega H^2)$, the rotation rate Ω and tank height H must also be measured. The rotation rate is measured by setting the rotation rate (in RPM divided by 40), $\Omega_{RPM}^{requested}$, from the fumehood computer and measuring the resulting the rotation of the stack using a Vernier Hall

Probe and Logger Pro Software, The resulting relation between the requested rotation rate and the actual rotation rate is given by:

$$\Omega_{RPM}^{real} = 1.0206\Omega_{RPM}^{requested} + 0.0011 \quad (27)$$

where Ω_{RPM}^{real} is the rotation rate in rotations per minute. The rotation rate used to calculate the Ekman number is then given by

$$\Omega = \frac{2\pi}{60}\Omega_{RPM}^{real}. \quad (28)$$

The tank height, H , is measured using a digital micrometer. These measurements permit a calculation of the Ekman number for each convection case.

N.6 Calculating the Temperature Drop Across the Fluid Layer

The temperature drop is measured using the top and bottom thermistors:

$$\Delta T_{fluid} = \frac{1}{6} \overline{\sum_{i=1}^6 T_i^{top}(t) - \sum_{i=1}^6 T_i^{bot}(t)} \quad (29)$$

where, again, the angled brackets indicate averages in time. Figure ??? shows the measurement of ΔT prior to time-averaging. Thus, we can now calculate the Rayleigh number for each convection run.

N.7 Calculating the Rayleigh Number

The Rayleigh number,

$$Ra = \frac{\alpha_T g \Delta T H^3}{\nu \kappa}, \quad (30)$$

is further dependent on g and ΔT . Gravitational acceleration is assumed to be $9.81 m s^{-2}$.

N.8 Calculating the Nusselt Number

In order to calculate the Nusselt number,

$$Nu = \frac{qH}{k\Delta T} = \frac{P}{A} \frac{H}{k\Delta T}. \quad (31)$$

The heat flux $q = P/A$, where P is heat power and A is the area through which that heat power flows, must be measured. As mentioned above, the heat power is measured as the electrical power supplied to

the heater. The area of the convection tank is calculated from the design drawings to be $A = 0.0314\text{m}^2$. These additional measurements allow us to calculate the fluids Nusselt number for each convection case. These data, Pr , E , Ra , and Nu , make up the bulk of the experimental results presented in this document, and are reported in the appendix for all convection cases in our publications.

O. Post Processing Data for Path to Magnetostrophy

The analysis of the acquisition text files should be performed in the following order

1. Calculate the raw power as measured by the PMU with $P_{raw} = IV$ using shunt voltage and divider voltage with proper multiplicative factors found in the forwarded Vincent email. Shunt voltage is multiplied by 297 and voltage divider voltage is multiplied by 37.
2. Calculate $P_{loss} = \Delta T_{insul} 2\pi H_{insul} k_{insul} / \ln((R_o + r_{insul})/R_o)$ where $H_{insul} = 8.5\text{cm}$ is the height of the insulation, $r_{insul} = 1.9\text{cm}$ is the thickness of the insulation, $k_{insul} = 0.036 \text{ W}/(\text{m-K})$ is the thermal conductivity of the insulation, and ΔT_{insul} is the temperature difference across the insulation using the thermistors placed on either side of the insulation. Find the two inner and outer thermistors at 30 and 210 degrees to do this.
3. Calculate the corrected power $P_{corr} = P_{raw} - P_{loss}$
4. Use P_{corr} to make conductive correction to the top and bottom lid, $\Delta T_{lid,corr} = P_{corr}(0.003)/(A_{fl}k_{cu})$ where 0.003 indicates that the thermistors in the lid are 3mm from the fluid interface. $A_{fl} = \pi(R_o - r_{sw})^2$ is the area of the copper lids in contact with the fluid layer where r_{sw} is the thickness of the tank sidewall, R_o is the outer radius of the cylindrical tank. R_o is most easily found by using a pi tape or measuring the outer circumference of the cylinder. The thermal conductivity of the copper lids is $k_{cu} = 390 \text{ W}/(\text{m-K})$.
5. Define new top and bottom fluid temps by subtracting and adding the correction $\Delta T_{lid,corr}$ respectively. The bottom fluid temp T_{bot} is $T_{bot,raw} - \Delta T_{lid,corr} = T_{bot,corr}$. The top fluid temp T_{top} is $T_{top,raw} + \Delta T_{lid,corr} = T_{top,corr}$.
6. Define the mean fluid temp and the temperature difference across the fluid layer by $\Delta T = T_{bot,corr} - T_{top,corr}$ and $T_{mean} = (T_{bot,corr} + T_{top,corr})/2$

7. Use T_{mean} to calculate the material properties using the appropriate equations.
8. You need to determine the heat conducted vertically through the sidewall. $P_{sw} = k_{sw}\Delta T A_{sw}/H$ where the vertical sidewall area $A_{sw} = \pi R_o^2 - \pi(R_o - r_{sw})^2$. The power transferred across the fluid is now $P = P_{corr} - P_{sw}$.
9. There is a correction to the raw rotation rate: $RPM = 1.0206RPM + 0.0011$ then $\Omega = 2\pi RPM/60$.
10. Calculate all relevant dimensionless parameters and fluid properties using Ω , P , ΔT , and T_{mean} .

References

- V. Bertin, A. M. Grannan, and J. M. Aurnou. Rotating convection in liquid gallium: Oscillations, Wall Modes and Turbulence. *Geophys. J. Int.*, In Prep., 2017.
- J. S. Cheng. *Characterizing convection in geophysical dynamo systems*. PhD thesis, University of California-Los Angeles, 2015.
- A. M. Grannan, V. Bertin, and J. M. Aurnou. Experimental studies of wall modes in rotating convection of liquid metals. *J. Fluid Mech.*, In Prep, 2017a.
- A. M. Grannan, T. Vogt, A. Aggarwal, E. K. Hawkins, and J. M. Aurnou. Behaviors and transitions along the path to magnetostrophic convection. *J. Fluid Mech.*, In Prep, 2017b.
- E. King. *An Investigation of Planetary Convection: The Role of Boundary Layers*. PhD thesis, University of California-Los Angeles, 2009.
- E. King and J. M. Aurnou. Turbulent convection in liquid metal with and without rotation. *Proc. Natl. Acad. Sci.*, 110:6688–6693, 2013.
- E. M. King and J. M. Aurnou. Magnetostrophic balance as the optimal state for turbulent magnetoconvection. *Proc. Natl. Acad. Sci.*, 112(4):990–994, 2015.
- D. R. Lide. 2001, CRC Handbook of Chemistry and Physics. *CRC Press*, 2000.